Journal of Sciences, Islamic Republic of Iran 16(1): 43-53 (2005) http://jsciences.ut.ac.ir
University of Tehran, ISSN 1016-1104

Magmatic and Metamorphic Fluids in Pegmatite Development: Evidence from Borujerd Complex, Iran

F. Masoudi[1,*] and B.W.D. Yardley[2]

[1] *Department of Geology, Faculty of Science, Tarbiat Moalem University, Tehran, Islamic Republic of Iran*
[2] *School of Earth Sciences, University of Leeds, Leeds, UK*

Abstract

The Borujerd complex of western Iran is composed of intrusions and their surrounding contact aureole, with, pegmatites and quartz veins. Pegmatites differ in mineralogy, origin and age, and two groups can be distinguished. The Older Pegmatites (about 120 Ma age) intruded contact metamorphic rocks from the early magmatic stage, while the Younger pegmatites (52-70 Ma age) formed during the late magmatic stage. Fluid inclusions from quartz veins, pegmatites and hornfelses have been studied using microthermometry, scanning electron microscopy, laser Raman spectroscopy and crush leach analysis to evaluate the source of fluids from which pegmatites formed. Host minerals of fluid inclusions in pegmatites are quartz and tourmaline, whereas in the hornfelses they are andalusite and quartz. Low salinity H_2O inclusions are common in the Older Pegmatites and quartz veins whereas high salinity H_2O inclusions occur in Younger Pegmatites. CO_2-H_2O fluid inclusions occur in Older Pegmatites and hornfelses, and in addition pure CO_2 inclusions are observed in some hornfelses. The distribution of the different types of fluid inclusions suggests that CO_2 fluids evaluated during metamorphism. The source of the carbon may be graphite which is present in hornfelses and the basement mica schists. Low salinity fluids in Older Pegmatites, quartz veins and hornfelses could have formed from low salinity late magmatic fluids. However, some mixing took place between magmatic fluids and metamorphic fluids to form CO_2-H_2O inclusions. High salinity magmatic fluids are only associated with Younger pegmatites and show low first ice melting temperature (−61.0 to −75.5°C), probably due to the presence of Ca.

Keywords: CO_2-H_2O Fluid inclusion; Iran; Pegmatite

1. Introduction

The coexistence of a saturated aqueous vapour phase with silicate melt is central to the models of Jahns and Burnham [9], Jahn [8] and Burnham and Nekvasil [2] for the formation of pegmatites and granitic pegmatites potentially record the history of late magmatic fluids [22].

* *E-mail: masoudi@tmu.ac.ir*

Tracing the evolution of fluids in pegmatites therefore has been a significant focus of research and there have been various studies on the chemical and physical properties of the aqueous phase and silicate melt [*e.g.* 10-15,25].

Like other highly polymerized melts (granitic compositions), presence of H_2O rich fluids during the formation of pegmatites is common, however the presence of CO_2 with H_2O in inclusions has also been reported [*e.g.* 1,22,24], although the source of CO_2 is not clear.

The goal of this study was to use fluid inclusions in Borudjerd complex pegmatites to evaluate the nature and source of the fluid or melt from which the pegmatites formed.

Among the pegmatites in Sanadaj Sirjan zone of metamorphic belt of Iran, those in the Borujerd complex are well developed. This study focused on this area because the outstanding exposure of the pegmatites offered unique sampling control, and because a variety of fluid inclusions is present.

Microscopic observation, conventional microthermometric measurements, studies of daughter minerals, crush-leach analyses and Laser-Raman analyses have been carried out on fluid inclusions found in pegmatites, quartz veins, and hornfelses.

2. Geological Setting

The Borujerd complex is composed of granitic intrusions with wide range of late magmatic product including pegmatites and quartz veins, and a well-developed aureole in pelitic country rocks (Fig. 1).

The studied area includes the north east corner of the Khoramabad quadrangle and is an area of Mesozoic schists, intrusive igneous rocks and pegmatites. The oldest known exposed rocks are Precambrian, but the intrusives are emplaced into metasediments of early Mesozoic age. Regional metamorphism reached a peak in the greenschist facies, but subsequent thermal metamorphism has occurred locally, associated with granitoid emplacement. Intrusions include granite, granodiorite and quartz diorite. This intrusive activity culminated with the emplacement of the pegmatites which exhibit a north-west trend.

Rb-Sr data [17] indicate that the first intrusive activity, which postdated low grade regional metamorphism, occurred in lower Cretaceous times (about 120 Ma). A large elongate granitic intrusion (Older Granites), which occupies most of the Borujerd complex, was formed during this stage. Following this, a series of post-tectonic intrusions (Younger Granites) were formed during the late Cretaceous-early Paleocene (52-70 Ma).

3. Pegmatites

In the Borujerd complex, two groups of pegmatites with different mineralogy, origin and age can be distinguished [16,17]. The Older Pegmatites, about 120 Ma in age, and the Younger Pegmatites, 52-70 Ma in age.

The Older Pegmatites

The Older Pegmatites are exposed in an area parallel to the northern margin of the Borujerd complex, where several hundred pegmatites occupy a distinct zone roughly 25 km long by 5 km wide with a northwesterly trend (Fig. 1). They mainly intrude contact metamorphic rocks as a series of linear veins and elongate bodies. The pegmatites are typically less than 100 m long and 30 m in thickness.

Many pegmatite bodies may be found, but those of most importance are exposed in a zone to the east of Kalejobe village, and in the southern flank of Koh-e-Malmir, which is an elongate mountain parallel to the Borujerd complex. Because of gentle topography on the northern flank of Koh-e-Malmir, the pegmatites are covered by alluvium in many places.

Individual pegmatites vary in their internal structure and composition, but there is a characteristic mineralogical signature exhibited by the majority. The Older Pegmatites are characteristically composed of quartz, muscovite, with microcline, albite, and perthite. Other minerals common to many pegmatites include tourmaline and garnet, which can often be found as large crystals, reaching up to 40 cm (length) and 3.5 cm (diameter) respectively. Also present in some pegmatites are andalusite, apatite, and zircon.

The Younger Pegmatites

The Younger Pegmatites comprise a few linear dykes hosted within the Younger Granites and are mainly located to the south of Malmir village (Fig. 1). The length of these pegmatites varies from a few metres to tens of metres with thickness up to 12 m. They are very coarse grained and contain mainly K-feldspar, albite, quartz, biotite, tourmaline and muscovite. The main pegmatite south of Malmir village (sample FM50) consists of 45% quartz, up to 45% K-feldspar and perthite, with biotite (<5%) and minor concentrations of albite, tourmaline and muscovite. The presence of biotite and lack of garnet distinguishes these pegmatites from the Older Pegmatites. The tourmalines are generally zoned particularly for Fe, Na, Mg, and Al.

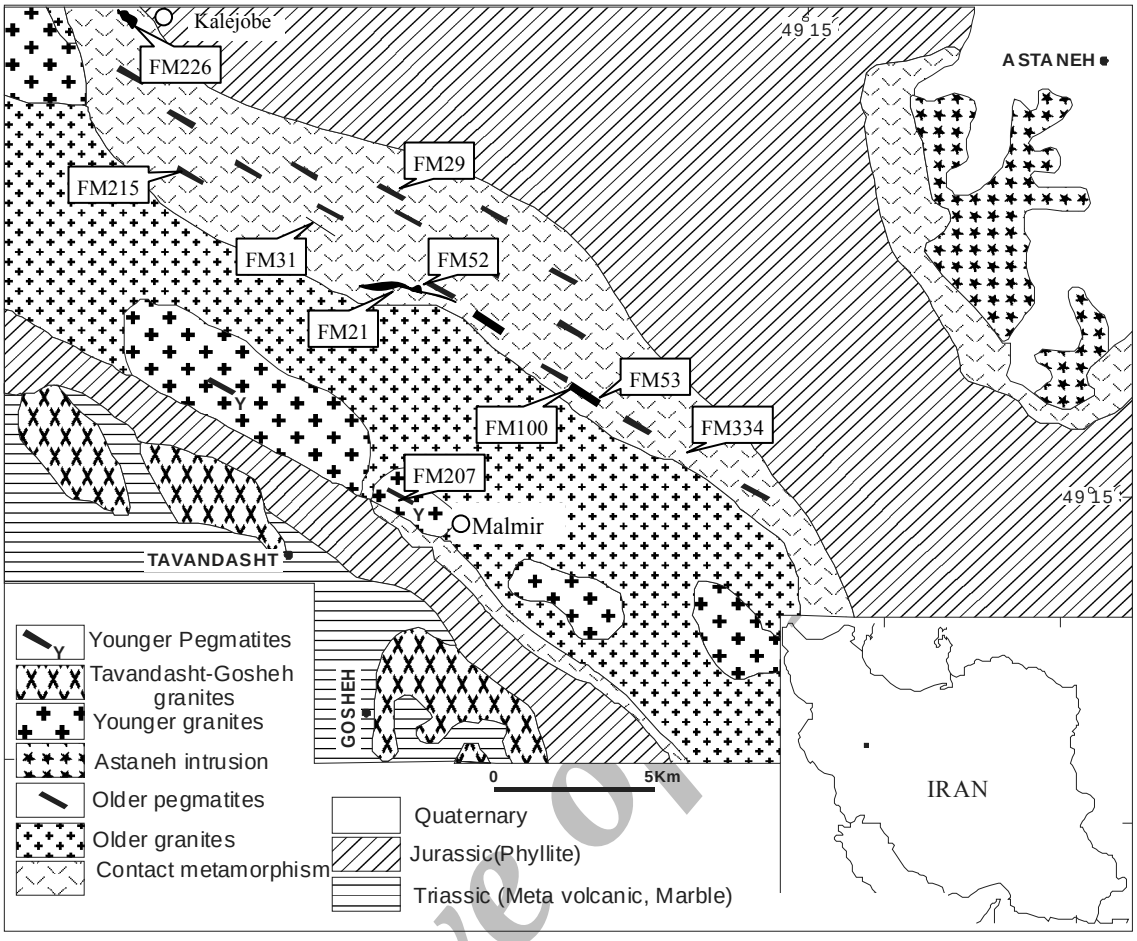

Figure 1. Simplified geological map of the Borujerd complex, showing the location of analyzed samples.

4. Studied Materials and Classifications

Fluid inclusions have been systematically studied in samples from quartz veins, pegmatites and hornfelses. The locations of the samples are shown in Figure 1. Host minerals in pegmatites are quartz and tourmaline, whereas in hornfelses they are andalusite and quartz.

Investigations indicate that most of the fluid inclusions in quartz crystals from quartz veins and pegmatite bodies are small (<7 μm) and secondary in origin, while the fluid inclusions in tourmaline are bigger (up to 50 μm) and both primary and secondary ones occur. Fluid inclusions have been observed along secondary fluid inclusion planes in quartz from quartz veins and pegmatitic rocks and in growth planes in tourmaline crystals.

In hornfelses, inclusions in quartz are pseudosecondary with diameters ranging from 3 μm to 7 μm, while inclusions in andalusite are primary in origin and inclusions with diameter ranging 7μm to 10μm are dominant.

Several fluid inclusion types were identified on the basis of phase assemblage at room temperature and host mineral. A classification scheme is given in Table 1.

5. Microthermometric Studies

Microthermometric characterization of fluid inclusions was performed on double polished wafers 300 μm thick for quartz samples and 200 to 250 μm thick (according to orientation) for tourmaline. In almost all instances the quartz samples were massive with no distinct crystal form, and as a result no choice of orientation was possible. In the case of tourmaline, the crystals were clearly zoned as well as being prismatic and so were sectioned perpendicular to the long axis, except where the wafer was not sufficiently transparent for microthermometric studies, where a section parallel to the c axis was used.

The heating-freezing stage used for all experimental work was a Linkam TMS 90.

Table 1. Classification scheme used for describing major fluid inclusion populations

Host rock	Host mineral	Inclusion type	Abbreviation used	Samples
Older pegmatites	Tourmaline	3 phase H_2O-CO_2	LV-C	FM53, FM100
Older pegmatites	Tourmaline	2 phase aqueous (low salinity)	LV	FM52, FM215, FM226
Older pegmatites	Quartz	2 phase aqueous (low salinity)	L"V	FM52, FM21
Quartz vein	Quartz	2 phase aqueous (low salinity)	L'V	FM29, FM31
Younger pegmatites	Tourmaline	2 phase aqueous ± Halite (high salinity)	LV, LV_h	FM207
Hornfels	Quartz	2 phase aqueous (low salinity)	L'"V	FM234
Hornfels	Quartz	2 phase CO_2	L_c-V_c	FM234
Hornfels	Andalusite	1 phase CO_2	L_c	FM234

The microthermometric measurements made were the first ice melting temperature (T_e), final ice melting temperature (T_{mice}), and homogenisation temperature (T_h) for low salinity 2 phase aqueous fluid inclusions. In the case of high salinity 2 phase inclusions, the temperature of hydrohalite melting (T_{mhy}) and for halite bearing inclusions, the temperature of homogenisation of halite (T_{hh}) were also measured. The melting temperature of CO_2 (T_{mCO2}), homogenisation of CO_2 liquid and vapour (Th_{CO2}), and clathrate melting point (T_{mclth}) were measured during the study of CO_2 bearing inclusions.

The measurements of T_{mice}, for inclusions with T_{mice}>−21°C, were converted to salinity (as weight % NaCl equivalent) using the equation of Bodnar [3].

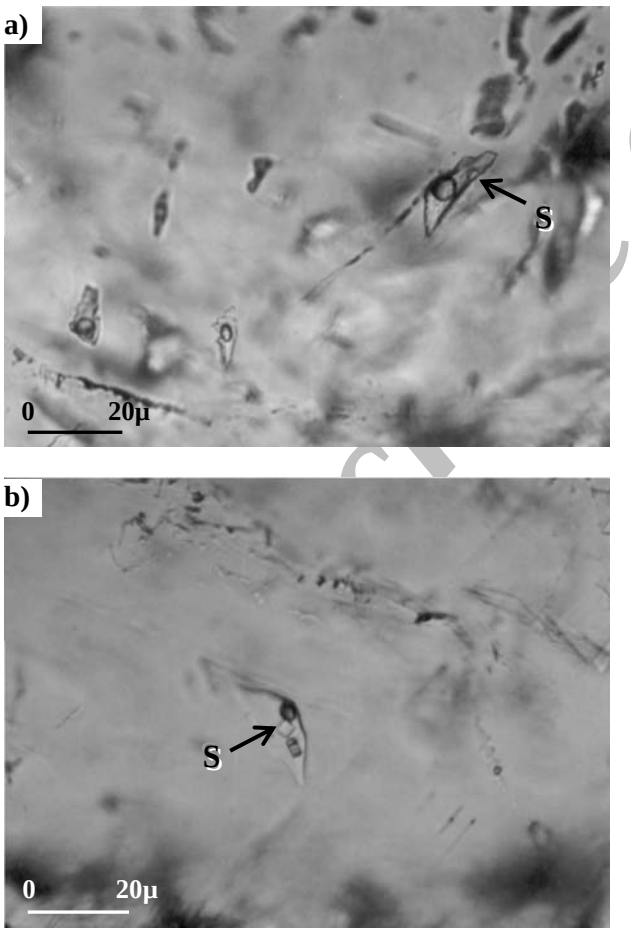

Figure 2. Transmitted light photomicrographs of primary (LV-LV_h) type inclusions, hosted by tourmaline, containing chloride solid phase. (a) sample FM207a (b) sample FM207b.

Fluid Inclusions in Tourmaline

In this study, fluid inclusions in tourmaline from different pegmatite bodies of Older Pegmatites (FM52, FM53, FM100, FM215, FM226) and Younger Pegmatites (FM207a, FM207b) have been examined. It seems that all tourmaline crystals from the same location exhibit similar features and contain only one type of inclusion. There are however significant differences between bodies. The fluid inclusion populations within tourmaline crystals can be classified into CO_2-bearing, aqueous and high salinity types (Fig. 2).

Tourmaline with CO_2-Bearing Inclusions from Older Pegmatites (LV-C)

Two samples were analysed from this group (FM100, FM53). Both primary and pseudosecondary CO_2-H_2O inclusions were present. Amongst the primary inclusions, negative crystal shapes were relatively common with inclusion diameters ranging from 15 µm to 50 µm. The pseudosecondary inclusions were much smaller in size (up to 15 µm), less abundant, and were more ragged in shape than the primary inclusions. However, they exhibited the same range of total homogenisation (T_h) and melting temperature of CO_2 (Th_{CO2}).

Most inclusions exhibit three fluid phases at 15°C, CO_2(l), H_2O(l) and CO_2(v), but the CO_2 content is variable. The volume ratio of CO_2/H_2O was found to be

within the range 1/1 to 1/3 in primary and pseudosecondary inclusions. However, some of the pseudosecondary inclusions contain only CO_2 and exhibit homogenisation to vapour.

CO_2-H_2O inclusions may exhibit homogenisation of the CO_2 to liquid or vapour (at Th_{CO2}), with total homogenisation (T_h) to the liquid. Only in one case did an inclusion homogenise to vapour at 321°C (FM53). Homogenisation of the CO_2 part (Th_{CO2}) is mostly in the temperature range of 12 to 22°C (Fig. 3a), while total homogenisation to the liquid phase occurs generally in the range 217 to 320°C (Fig. 3b). Melting temperatures of CO_2 (Tm_{CO2}) were between −59.2 and −57.3°C and clathrate melting temperatures between 3.7 and 8.4°C. Tm_{CO2} is significantly lower than the melting temperature of pure CO_2 (−56.6°C), indicating the presence of volatile compounds other than CO_2.

Some aqueous primary inclusions are also present with an ice melting temperature range of −7.1 to −10.14°C (10.61 to 14.36 weight % NaCl equivalent), total homogenisation of 260 to 301°C and first ice melting temperature (T_e) range of −21.5 to −34.0°C.

Tourmaline with Aqueous Fluid Inclusions from Older Pegmatites (LV)

Aqueous fluid inclusions are abundant in tourmaline crystals from NW of the area (FM215), the Hajibeg Mine (FM52) and east of Kalejob village (FM226). They occur along tourmaline growth zones and formed during primary growth of the tourmaline crystals. Inclusion diameters are from 10 µm to 30 µm and first ice melting temperature (T_e) range from −26.0 to −31.5°C with total homogenisation (T_h) to the liquid phase at temperatures from 212 to 320°C (Fig. 3c). According to the temperature of ice melting, salinity generally varies between 8 to 14 weight % NaCl equivalent (Fig. 3d). However, two groups of inclusions have been distinguished in sample FM52: 1) primary inclusions with T_{mice} from −5.7 to −8.8°C (8.81 to 12.62 weight % NaCl equivalent) located in the core and central parts of the crystals; and 2) inclusions with T_{mice} ranging from −9.9 to −12.9°C (13.83 to 16.80 weight % NaCl equivalent) which are concentrated in the outer zones and rim of the crystals as primary inclusions, or occur in the central parts as pseudosecondary inclusions.

Tourmaline with High Salinity Inclusions from Younger Pegmatites (LV-LV_h)

High salinity fluids are observed in tourmaline from Younger Pegmatites and are introduced here as (LV-LV_h) type (FM207). They occur as primary inclusions, with or without halite cubes, which are generally elongated and are up to 50µm in length. The first ice melting temperature (T_e) ranges from −61.0 to −74.5°C. Most NaCl rich inclusions exhibit hydrohalite melting (T_{mhy}) from −31.0 to −35.8°C. The temperature of ice melting generally ranged from −27.2 to −39.5°C. Total homogenisation is 220 to 336°C for inclusions with halite, but ranges from 208 to 300°C for inclusions without halite. Histograms of T_h and T_{mice} are given in Figure 4.

Halite-bearing inclusions also have two-fluid phases at room temperature. Ice melted in the range −40.0 to −43.3°C in halite-bearing inclusions. The halite cube melts at around 171 to 235°C, generally before total homogenisation (T_h).

Fluid Inclusions in Quartz

Aqueous Fluid Inclusions in Quartz from Quartz Veins (L'V) and Pegmatites (L''V)

Aqueous fluid inclusions are abundant along secondary fluid inclusion planes (FIP) in quartz from quartz veins (L'V) and pegmatite bodies (L''V). Most inclusions exhibit only two phases at room temperature, normally H_2O(V) and H_2O(L). The diameter of inclusions is typically <6 µm, and shapes are sub-rounded. Homogenisation is mostly to the liquid, in the range 150 to 295°C for L'V (FM31, FM29) and 120 to 325°C for L''V inclusions (FM52, FM21). Histograms of T_h are given in Figure 4.

Ice melting temperature range from −4.8 to −8.8°C (7.59 to 12.62 weight % NaCl equivalent) for both groups (Fig. 4).

Aqueous Fluid Inclusions in Quartz from Hornfels (L'''V)

Most inclusions in this group are secondary and water-rich. The host quartz formed during contact metamorphism. Inclusions are rounded with uniform size (4-7 µm) and exhibit total homogenisation (T_h) to the liquid in the range of 190 to 295°C (FM234). The salinities of these inclusions are moderate, with values ranging from 9.08 to 15.17 weight % NaCl equivalent.

CO_2-Rich Inclusions in Quartz from Hornfelses (Lc-Vc)

A small number of pseudosecondary CO_2-rich inclusions with irregular shapes and diameters ranging from 3 µm to 7 µm also occur in quartz. This group of inclusions shows only one fluid phase at room temperature. The melting temperature of CO_2 (Tm_{CO2}) ranges from −59.3 to −61.8°C, *i.e.* is lower than that of pure CO_2, indicating the presence of additional volatile components, such as CH_4 and N_2. Homogenisation is mostly to liquid, ranging from −5.1 to +15.0°C. This wide range of variation may also be the result of chemical heterogeneity.

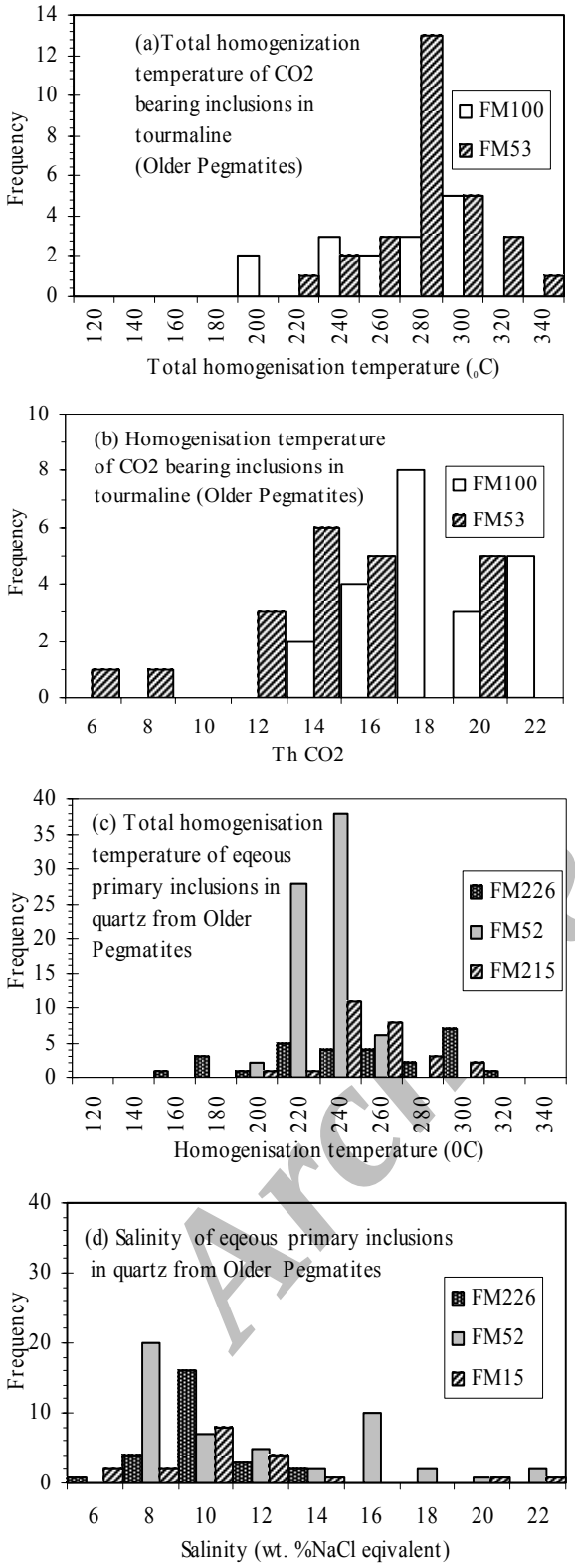

Figure 3. Homogenization temperature of CO_2 (a), and total homogenization (b) of CO_2 bearing inclusions from Older Pegmatites. Total homogenization temperature (c) and salinity of aqueous inclusions in tourmaline from Older Pegmatites.

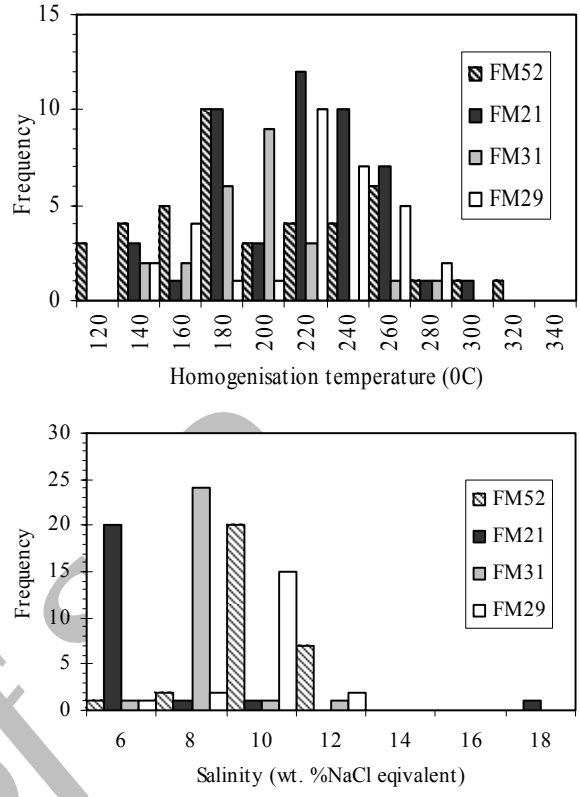

Figure 4. Homogenization and salinity of secondary inclusions in quartz from quartz veins and pegmatites.

Fluid Inclusions in Andalusite (Lc)

Irregular primary CO_2-rich inclusions with diameters ranging from 5 μm to 10 μm have been observed within andalusite from hornfelses (FM234). The presence of various mineral and carbon inclusions in andalusite makes it very difficult to find good fluid inclusions in andalusite at room temperature, hence only 6 inclusions were measured. For each, the inclusion has been cooled to −100°C to identify the CO_2 phase. The melting temperature of CO_2 ranges only from −58.8 to −59.0°C. CO_2 homogenisation is to liquid, at temperatures in the range 18.3 to 19.2°C.

6. Studies of Daughter Minerals

Scanning Electron Microscopy (SEM) has been used to examine opened fluid inclusions in tourmaline for the presence of daughter minerals, in samples from Older Pegmatites (FM52, FM215, FM226) and Younger Pegmatites (FM207). Because of the small size of fluid inclusions within quartz (< 7 μm) these were not suitable for study. In addition, an X-ray analyser has provided qualitative compositional spectra for daughter

phases. By combining the crystallographic observations with the x-ray spectra, a relatively precise identification of the daughter minerals has been achieved.

The relative abundance of daughter phases within the fluid inclusions varies from sample to sample, but as an approximation only 8% of all inclusions observed contained a daughter phase. In samples from Younger Pegmatites this percentage was considerably higher, and up to 30% of fluid inclusions contained a daughter phase.

Tourmaline crystals were prepared for investigation by cutting them into square-based columns with a width of approximately 0.75 cm and a height of between 3 cm and 6 cm. It was found necessary to put some of the more friable samples (FM52, FM215) into a square-based mould and fill it with resin to make a rigid column. The columns were broken immediately prior to carbon coating.

The most common daughter minerals found in Older Pegmatites are muscovite, alkali feldspars and quartz, and in Younger Pegmatites are muscovite, alkali feldspars chlorides, and quartz. The chloride crystals exhibit a euhedral cubic habit and were only observed under the optical microscope.

7. Crush-Leach Analyses of Fluid Inclusions

Salt-rich fluid inclusions in Younger Pegmatites (FM207) show a low eutectic point (−70 to −65°C). Li or Ca might be the cause of the low eutectic point. Bulk crush-leach analyses for both anions and cations (Li, Mn, K, Ba, Zn, Fe, Ca, Mg, Al, Cu, Sr, Na, P, S- as SO_4^{2-} and Br, Cl, F) have been obtained from fluid inclusions within quartz and tourmaline to reconstruct the bulk fluid chemistry of inclusions.

The basic method of sample preparation, cleaning and crushing is a modified version of that originally proposed by Bottrell *et al.* [4], refined by Yardley *et al.* [26].

Three different analytical techniques have been used. The solutions analyzed for cations using ICP (Na, K, Ca, Mg, Fe, Mn, Al, Li, Sr, Ba, Cu, Zn, B) and AA-FES (Na, K), and for anions (F^-, Cl^-, Br^-, SO_4^{2-}) using a Dionex Ion Chromatograph.

In total 11 samples were analyzed, and leachate analyses are presented in Table 2. The high K/Na ratios of most analyses are indicative of a high-T (magmatic) origin. Note that since Ca>>Li, the presence of Ca is a more likely cause of the low initial melting points (T_e).

8. Laser-Raman Analyses

The mol% of components in the gas phase for gas-bearing inclusions in tourmaline (FM100, FM53) were obtained by Raman spectroscopy. 14 inclusions of type LV-C, 3 inclusions of type (LV-LV_h) and 2 inclusions of type LV have been examined by laser Raman spectroscopy at CREGU, Nancy, France. In 4 of the 14 tourmaline inclusions of type LV-C, and all inclusions of types (LV-LV_h) and type LV, the signal from inclusions was too weak for Raman analysis. The remaining 10 inclusions produced strong signals for CO_2, CH_4 and N_2. H_2S was scanned for but found to be below the detection limits.

The Raman spectra were recorded on a Dilor X-Y multichannel analyzer, optically coupled to an Olympus microscope (BH2) with X80 long distance objective. The 514 nm exciting radiation is provided by a Spectra Physics 2020-50 Ar laser.

The volume fraction of liquid phase has been estimated from the diagrams of [20] fluid inclusions with a visible liquid phase.

In order to calculate the composition and total density of fluid inclusions, the molar volume of the volatile phase was determined from diagrams of Thiery *et al.* [23], based on measured compositions in the CO_2-CH_4 and CO_2-N_2 systems, microthermometric results and Raman spectroscopic data (Table 3).

The composition and density of fluid inclusions were calculated from the equation of Bowers and Helgeson [5] and Dubessy *et al.* [6] using a computer program developed at CREGU.

9. Discussion

Origin of Fluids

The distribution of fluid inclusion types is summarised in Table 4. This complements Table 1, but all H_2O-low salinity inclusion types are considered as one group. CO_2, CO_2-H_2O, H_2O-low salinity and H_2O-high salinity fluid inclusion types are present. The following fluid sources have been suggested for the formation of different fluid inclusion groups.

1) Metamorphic fluids

CO_2-rich fluids are less likely to have evolved from differentiated granitic magma, because of the very low CO_2 solubility in such magma [21]. Metamorphic rocks are most closely associated with CO_2 bearing fluids [18], which are therefore best explained as metamorphic fluids. The source of the carbon may be graphite, which is present in hornfelses and the basement mica schists. During contact metamorphism, reheating of C-rich rock yields volatile-bearing fluids as a result of graphite water reaction.

2) Low salinity fluids

Table 2. Blank corrected data (in ppm) of fluid inclusions analyzed by crush leach method. Dashed lines (----) indicate no analysis for the element

Type	**(LV-LV$_h$)**			**LV-C**			**LV**	**L'V**	
Sample	FM207 I	FM207 I	FM207 II	FM100	FM53	FM53	FM52	FM29	FM31
	Tourmaline	Quartz	Quartz	Tourmaline	Tourmaline	Quartz	Tourmaline	Quartz	Quartz
Na	----	28790.71	73314.57	----	----	46230.00	----	27336.14	29036.56
K	----	31445.50	62540.52	----	----	15381.25	----	26521.87	7499.60
Li	----	128.16	197.63	----	----	345.00	----	58.16	20.91
Zn	----	9.15	159.38	----	----	0.00	----		202.13
Ba	----	96.12	248.63	----	----	83.38	----	325.71	493.47
Mn	----	553.84	1032.78	----	----	140.88	----	668.86	1143.06
Fe	----	2375.58	3754.98	----	----	1265.00	----	1442.42	315.32
Mg	----	659.12	395.26	----	----	310.50	----	284.99	1190.46
Ca	----	36269.89	109168.6	----	----	38217.38	----	25117.26	17637.31
Cu	----	100.70	586.52	----	----	31.63	----	133.77	15.33
Sr	----	494.34	1147.53	----	----	540.50	----	564.17	340.13
F	27137.27	3890.64	36402.28	46905.93	46160.20	2846.25	78042.80	10701.81	1658.83
Cl	86828.09	86829.86	86829.95	66770.00	66769.96	48558.75	54629.96	66769.98	54630.00
Br	271.08	47.60	98.18	1118.40	443.25	147.78	67.53	95.39	73.74
SO_4^{2-}	8918.32	1190.08	5673.91	39227.38	49971.60	4945.00	12785.73	29429.97	850.33

Table 3. Microthermometric data and Raman microspectroscopy results for analyzed LV-C inclusion type in tourmaline from Older Pegmatites

Sample	**FM100**	**FM100**	**FM100**	**FM100**	**FM100**	**FM100**	**FM100**	**FM100**	**FM53**	**FM53**
Aqueous phase vol%	75	70	85	5	60	55	75	80	80	75
$TmCO_2$	−58.4	−58.4	−58.4	−58.5	−58.7	−58.6				
Te		−38.5	−40.0	----						−35.4
Tmice		−16.8	−13.3	----			−13.0	−13.0	−14.5	−12.8
Tmclath	+5.7	+5.2	−8.5	----	+3.7	+3.5	−7.0	−12.0	−12.0	−7.0
$ThCO_2$	19.7L	12.0L	----	26.3L	14.1L	15.2L	----	----	----	----
					Reconstructed fluid composition (mol%)					
H_2O	81.54	78.3	88.78	19.40	77.94	75.61	88.86	89.00	87.95	88.99
NaCl	5.14	6.12	9.76	0.88	4.24	4.45	9.33	9.81	10.78	9.22
CO_2	12.80	15.3	1.39	67.24	16.23	17.23	1.66	1.17	1.19	1.65
N_2	0.24	0.00	0.04	10.62	1.24	2.07	0.12	0.01	0.04	0.10
CH_4	0.28	0.28	0.006	1.87	0.35	0.64	0.02	0.00	0.011	0.02
Density	1.09	1.09	0.785	0.49	0.94	0.90	0.70	0.73	0.728	0.70

Table 4. Distribution of fluid inclusion types

Host rock	Host mineral	CO_2 (L_c-V_c), (L_c)	CO_2-H_2O (LV-C)	H_2O-low salinity (LV), (L'V), (L''V), (L'''V)	H_2O-high salinity (LV, LV_h)
Older pegmatites	Quartz			*	
	Tourmaline		*	*	
Younger pegmatites	Tourmaline				*
Vein Quartz				*	
Hornfels	Matrix Quartz	*	*		
	Matrix Andalusite	*			

Two phase aqueous inclusions in Older Pegmatites, quartz veins and hornfelses show moderate salinity (7-13 weight% NaCl). Such fluids could represent late magmatic fluids. Metamorphic reactions also could release H_2O low salinity fluids.

3) High salinity magmatic fluids

H_2O-high salinity primary inclusions occur only in Younger Pegmatites. The fluids show a low eutectic point (−70 to −65°C), probably due to the presence of Ca. This type of inclusion is considered to be associated with magmatic conditions and in addition to topaz and mica, they commonly contain oxides, fluorides, chlorides and borates as solid phases [7].

Relationships between Fluid Inclusion Types

Origins and relationships between different fluids are summarised in Figure 5. Older Pegmatites and hornfelses were formed in the same stage in the early Cretaceous but Younger Pegmatites crystallized during late Cretaceous-early Paleocene [17]. Because of the difference in age, the physical and chemical trapping conditions of fluids were different in Older Pegmatites and Younger Pegmatites.

Older Pegmatites and Hornfelses

The distribution of fluid inclusion types in Table 4 indicate that CO_2-H_2O type occurs in Older Pegmatites and hornfelses, while CO_2 inclusions were only observed in hornfelses. H_2O-low salinity inclusions are common in Older Pegmatites and quartz veins

Tourmaline crystals which contain only aqueous inclusions (LV) demonstrate that pegmatites could grow in a purely aqueous system. However other tourmaline crystals contain CO_2-bearing inclusions, indicating mixing with a CO_2 fluid from a different source, such as the surrounding rocks.

C-rich metamorphic fluids were trapped as primary and pseudosecondary fluid inclusions in andalusite crystals and mixed with pegmatite-forming fluids, resulting in aqueous fluids in the pegmatitic system being enriched in CO_2 (LV-C inclusions in tourmaline) and CO_2 bearing fluids in hornfelses being mixed with aqueous fluids and then trapped in quartz crystals in hornfelses. The wide range of variations in CO_2% (Table 3) for fluid inclusions in tourmaline and temperature of CO_2 homogenisation for fluid inclusions in quartz crystals from hornfelses (−5.1 to 15.0°C) and CO_2 inclusions within tourmalines from pegmatites confirm such mixing.

The range of salinity for fluid inclusions in hornfelses and pegmatites are the same, which suggests that H_2O in hornfelses may be the magmatic fluid. The presence of magmatic fluids is also indicated by the mineralogy of the pegmatites. Large crystals of tourmaline are common in the Older Pegmatites (up to 35% in FM52) and the source for F, B and Li was likely the low salinity magmatic fluid rather than metamorphic fluids.

H_2O is also expected to be released during the reactions between minerals during metamorphism. However, primary fluid inclusions in andalusite are pure CO_2 inclusions. It is possible that the original H_2O content of these inclusions has reacted with andalusite to produce hydrous phyllosilicates during cooling.

Younger Pegmatites

Low eutectic salt-rich fluids with muscovite, alkali feldspars, chlorides and quartz daughter minerals occur in tourmaline crystals from Younger Pegmatites.

The inclusions were formed from magmatic fluids.

10. Conclusions

Fluid inclusions in pegmatites from the Borujerd Complex record the metamorphic and magmatic fluid activities during the formation of pegmatites in this area.

The distribution of fluid inclusion types indicates that magmatic and metamorphic fluids were present during the crystallization of Older Pegmatite. However, in the

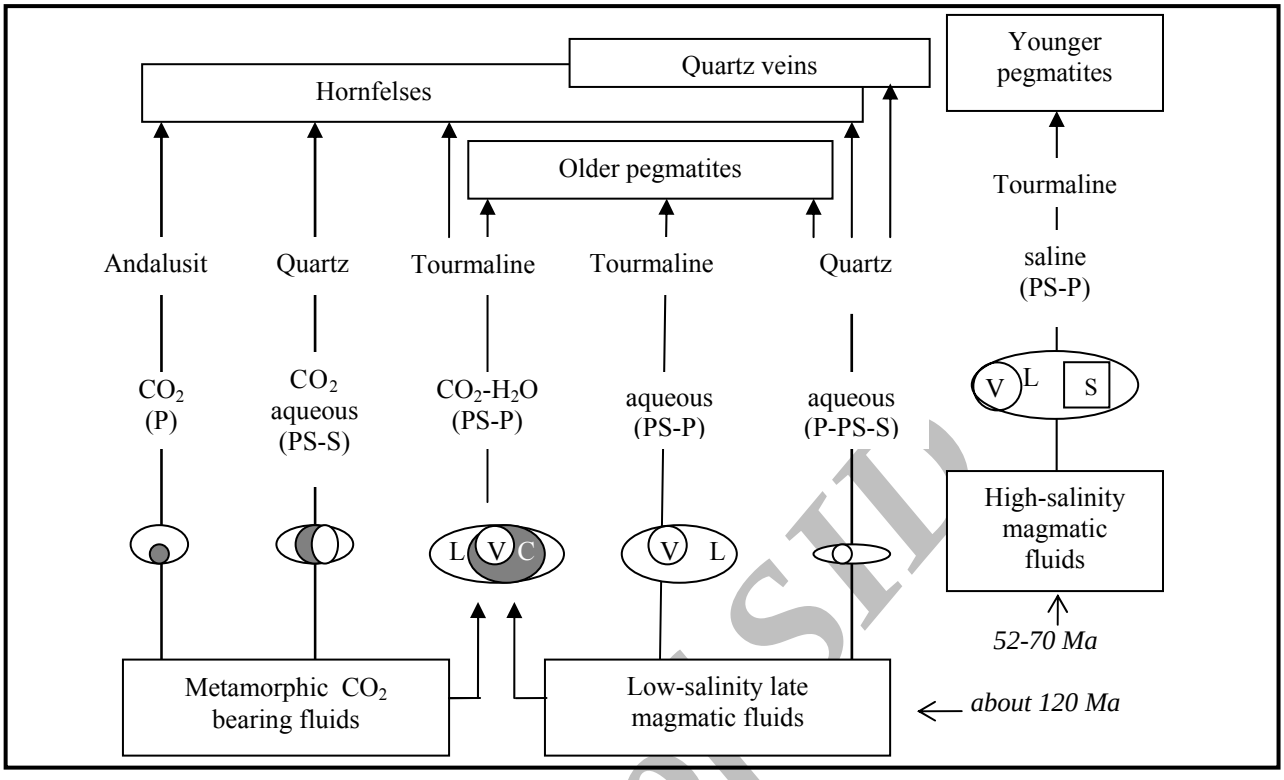

Figure 5. Origins and relationships between different fluids. P=primary, PS=pseudosecondary, S=secondary.

Borujerd complex Younger Pegmatites are the last products of magmatism [16]. Younger Granites and their associated Younger Pegmatites are mainly intruded in Older Granites and were not contaminated by CO_2 bearing fluids during migration through previously crystallized granite in an isolated magmatic system

Thomas *et al.* [24] reported migration of late magmatic fluids to country rocks to form H_2O-CO_2-CH_4-NaCl fluids in metasomatic tourmaline. Tourmalization is common in Borujerd Complex aureole [16] and is more abundant in the hornfelses close to the Older Granites. This feature, suggests migration of magmatic fluids in the metamorphic aureole of the Borujerd Complex. However, presence of CO_2 bearing fluid in Older Pegmatites suggests that metamorphic fluids might also contribute to the formation of the Older Pegmatites which may not simply record the history of late magmatic fluids.

Acknowledgments

The authors would like to thank the staff and management of CREGU in France for allowing accesses and training to undertake Raman spectroscopic analyses.

References

1. Beurlen H., Silva M.R.R., and Castro C. Fluid inclusion microthermometry in Be- Ta- (Li-Sn)-bearing pegmatites from the Borborema Province, Northeast Brazil. *Chem. Geol.*, **173**: 107-123 (2000).
2. Burnham C.W. and Nekvasil H. Equilibrium properties of granitic magmas. *Amer. Mineral.*, **71**: 239-263 (1986).
3. Bodnar R.J. Revised equation and table for freezing point depressions of H_2O-salt fluid inclusions (abst.) PACROFI, Fourth Biennial Pan-American Conference on Research on Fluid Inclusions, Program and Abstracts, Lake Arrowhead, Ca, **4**: 15 (1992).
4. Bottrell S.H., Yardley B.W.D., and Buckley F. A modified crush-leach method for the analysis of fluid inclusion electrolytes. *Bull. Mineral.*, **111**: 279-290 (1988).
5. Bowers T.S. and Helgeson H.C. Calculation of the thermodynamic and geochemical consequences of nonideal mixing in the system H_2O-CO_2-NaCl on phase relations in geologic system: Equation of state for H_2O-CO_2-NaCl at high pressure and temperatures. *Geochim. Cosmochim. Acta*, **47**: 1247-1275 (1983).
6. Dubessy J., Boiron M.C., Moissette A., Monnion C., and Sretenskaya N. Determination of water, hydrates and pH in fluid inclusions by micro-Raman spectrometry. *Eur. J. Mineral.*, **4**: 885-894 (1992).
7. Foord E.E., London D., Kampf A.R., Shigley J.E., and Snee L.W. Gem-bearing pegmatites of San Diego

County, California. In: M.J. Walawender and B.B. Haanan (Eds.), *Geological Excursions in Southern California and Mexico*, p. 128-146. Geological Society of America Guidebook, Boulder, Colorado (1991).
8. Jahns R.H. Internal evolution of pegmatite bodies. In: P. Cerny (Ed.), *Granitic Pegmatites in Science and Industry*. Mineralogical Association of Canada Short Course Handbook 8, 293-327 (1982).
9. Jahns R.H. and Burnham C.W. Experimental studies of pegmatite genesis: A model for derivation and crystallization of granitic pegmatites. *Econ. Geol.*, **64**: 843-864 (1969).
10. London D. Experimental phase equilibria in the system $LiAlSiO_4$-SiO_2-H_2O; A petrogenetic gride for lithium rich pegmatites. *Amer. Mineral.*, **69**: 995-1004 (1984).
11. London D. Magmatic-hydrothermal transition in the Tanco rare-element pegmatite: Evidence from fluid inclusions and phase equilibrium experiments. *Ibid.*, **71**: 376-395 (1986).
12. London D. The application of experimental petrology to the genesis and crystsllization of granitic pegmatites. *Can. Mineral.*, **30**: 499-540 (1992).
13. London D. and Burt D.M. Lithium aluminosilicate occurrences in pegmatite and the lithium aluminosilicate phase diagram. *Amer. Mineral.*, **67**: 483-493 (1982).
14. London D., Morgan G.B. VI, and Hervig R.L. Vapor-undersaturated experiments with Macusani glass + H_2O at 200 MPa, and the internal differentiation of granitic pegmatites. *Cont. Mineral. Petrol.*, **102**: 1-17 (1989).
15. Manning D.A.C. The effect of fluorine on liquidus phase relationships in the system Qz-Ab-Or with excess water at 1kb. *Ibid.*, **76**: 206-215 (1981).
16. Masoudi F. *Contact metamorphism and pegmatite development in the region SW of Arak, Iran*. Ph.D. Thesis, The university of Leeds (1997).
17. Masoudi F., Yardley B.W.D., and Cliff R.A. Rb-Sr geochronology of pegmatites, plutonic rocks and a hornfels in the region south-west of Arak, Iran. *J. Sci. I. R. of Iran*, **13**(3): 249-254 (2002).
18. Nabelek P.I. and Wilke M. Carbonic fluid production during regional and contact metamorphism in the Black Hills, USA. Goldschmidt Conference Abstracts (2002).
19. Norton J.J. Origin of lithium-rich pegmatitic magmas, southern Black Hills, South Dakota. *Geol. Soc. Am.*, Abstr. Programs, 34, 221 p. (1981).
20. Roedder E. Composition of fluid inclusions. *U.S. Geol. Survey Prof. Paper*, 440JJ, 164 p. (1972).
21. Shilobreeva S.N. and Kadik A.A. Carbon and its volatile compounds in silicate melts and crystals: Experimental data. Proc. First Indo-Soviet Workshop on Exp. Mineral. Petrol., New Delhi, 39-41 (1987).
22. Smerekanicz J.R. and Dudas F.O. Reconnaissance fluid inclusion study of the Morefield pegmatite, Amelia County, Virginia. *Amer. Mineral.*, **84**: 746-753 (1999).
23. Thiery R., Vidal J., and Dubessy J. Phase equilibria modelling applied to fluid inclusions: liquid-vapour equilibria and calculation of the molar volume in the CO_2-CH_4-N_2 system. *Geochim. Cosmochim. Acta*, **58**: 1073-1082 (1994).
24. Thomas A.V., Pasteris J.D., Bray C.J., and Spooner T.C. H_2O-CH4-NaCl-CO2 inclusions from the footwall contact of the Tanco granitic pegmatite: Estimates of internal pressure and composition from microthermometry, laser Raman spectroscopy, and gas chromometry. *Ibid.*, **54**: 559-573 (1989).
25. Whitworth M.P. and Rankin A.H. Evolution of fluid phases associated with lithium pegmatites from SE Ireland. *Mineral. Mag.*, **53**: 271-284 (1989).
26. Yardley B.W.D., Banks D.A., Bottrell S.H., and Diamond L.W. Post-metmorphic gold-quartz veins from N.W. Italy: the composition and origin of the ore fluid. *Ibid.*, **57**: 407-422 (1993).